POCL3-BASED CO-DIFFUSION PROCESS FOR N-TYPE BACK-CONTACT BACK-JUNCTION SOLAR CELLS

R. Keding[1,2], M. Hendrichs[1], D.Stüwe[1], M. Jahn[1], C. Reichel[1], D. Borchert[1], A.Wolf[1], H. Reinecke[3], D.Biro[1]
[1]Fraunhofer Institute for Solar Energy Systems, Heidenhoferstraße 2, D-79110 Freiburg, Germany
[2]Freiburg Material Research Center, University of Freiburg, Stefan-Maier-Straße 21, D-79104 Freiburg, Germany
[3]Institute for Microsystems Engineering, University of Freiburg, Georges-Köhler-Allee 103, D-79110 Freiburg, Germany

ABSTRACT: Back-contact back-junction (BC-BJ) solar cells have been developed to meet the following objectives: *process simplification* by $POCl_3$ based co-diffusion steps and *efficiency improvement* independent of the co-diffusion setup. In general, the process sequence is industrially feasible, requires not more than one temperature step (co-diffusion), and implements only industrially available patterning technologies. The process simplification is obtained by introducing a sophisticated co-diffusion process which combines solid diffusion sources with $POCl_3$. Compared with BC-BJ cells featuring solid diffusion sources at the front side, the number of process steps could be decreased. Solar cells based on this process simplification feature conversion efficiencies up to 20.5 %. The efficiency improvement is obtained by integrating an improved B-source, by adjusting the material properties and by changing the pattern of the contact openings. BC-BJ cells based on the latter cell improvements feature conversion efficiencies up to 21.6 %. The efficiency improvement is transferable to cells based on the regarded process simplification featuring $POCl_3$ as gaseous diffusion source.
Keywords: *n*-type, back contact, co-diffusion

1 INTRODUCTION

By aiming at industrial solar cell fabrication, the ratio of costs to watt peak has to be lowered [1]. This can be achieved by decreasing the overall solar cell manufacturing costs including material, process and module assembly, and/or increasing solar cell efficiency [2]. One very promising approach for decreasing optical losses on the front side of the solar cell and, thus, increasing the solar cell efficiency is to electrically contact solar cells only at the rear side. Based on this approach, so called back-contact back-junction (BC-BJ) solar cells already showed efficiencies higher than 24% [3]. To benefit from the high efficiency potential, the process chain of the sophisticated solar cell must be kept as short as possible.
Within this work, a potentially low-cost BC-BJ base line process is demonstrated, by applying an advanced co diffusion process. This advanced process enables the simultaneous diffusion of all the required highly doped surfaces in only one single thermal treatment. Besides that, all cells are prepared under semi-industrial conditions in the PV-TEC (Photovoltaic Technology Evaluation Center, [4]) on Czochralski (Cz) grown silicon wafers featuring an *n*-type base doping.

2 BASE LINE PROCESS

Within this section, the simplified BC-BJ base line processes with and without phosphoryl chloride ($POCl_3$) during diffusion are introduced. Therefore, the process lines of cells without (A, high process effort) and with $POCl_3$ (B, low process effort) are compared (Figure 1).
The process lines start with the formation of a single sided texture in an alkaline solution applying a single sided mask. Afterwards, a phosphorus-doped silicate glass (PSG) is deposited on the rear surface by means of plasma enhance chemical vapour deposition (PECVD). In case of process route A, also the front surface features a PSG-layer for front surface field (FSF) formation. The P-concentration incorporated within the PSG layers can be varied by e.g. adjusting the gas flows during PECVD [5].

Then, an inkjet-printed etch mask combined with wet chemical processes [6] enables patterning of the PSG-layer.

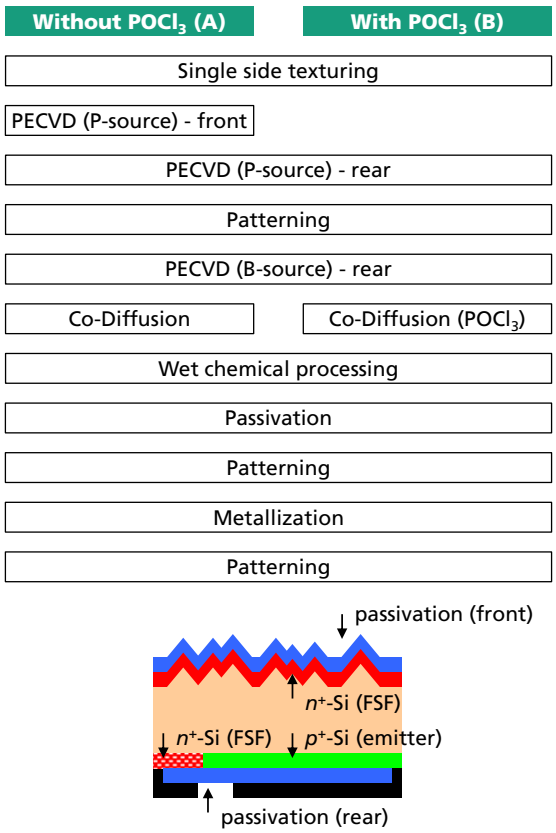

Figure 1: Base line process used for BC-BJ processing of cells with FSF formed by PECVD PSG source (left) and by $POCl_3$ diffusion (right).

Subsequently, the deposition of boron-doped silicate glass (BSG) is carried out by means of PECVD [7, 8]. The configuration of the diffusion sources allows for a simultaneous diffusion of all the required doped surfaces in one single thermal treatment. The so called

co-diffusion process, thus, enables a high potential in saving process costs. After co-diffusion, the doped layers are removed by wet chemical etching. The base line process finishes with the deposition of the front passivation stack consisting of SiO_xN_y/SiN_x [9] and rear side passivation stack consisting of Al_2O_3/SiN_x [10]. Inkjet masking and etching forms local openings at the rear side followed by evaporation of an aluminium silicon alloy (Al-Si). Again, inkjet masking is applied for structuring the interdigitated grid.

Figure 2 depicts a top view on the rear side of the processed large-sized (156 mm edge length) wafers integrating 25 small-sized BC-BJ solar cells. Since large-sized BC-BJ solar cells without diffused busbars are aimed at, the small-sized cells are characterized with a busbar shading aperture featuring an area of 4 cm^2.

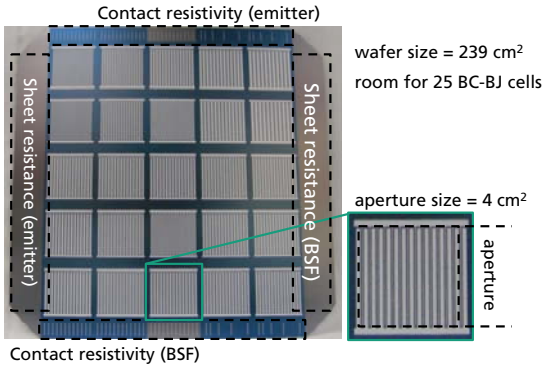

Figure 2: Top view on the processed rear side of a wafer integrating 25 small-sized BC-BJ solar cells.

3 PROCESS SIMPLIFICATION

3.1 Motivation and approach

Within this work, the process simplification is performed by using $POCl_3$ as gaseous diffusion source during the co-diffusion process. As highlighted in Figure 1, the introduction of a gaseous diffusion source allows for the omission of a complete PECVD process step and, hence, for a reduced number of process steps. However, co-diffusion processes with $POCl_3$ as gaseous diffusion source in combination with solid diffusion sources exhibit a high complexity. For example, unnecessarily high gas flows during diffusion might have a drastic impact on solid diffusion sources. The first objective is to realize P-doped surfaces with doping-levels suitable for FSF applications [11]. The second objective is to provide an atmosphere which does not oxidize the interface between pre-deposited solid diffusion sources located on the rear side of the solar cell and silicon.

A diffusion process with two temperature plateaus is introduced. During the first temperature plateau $POCl_3$, oxygen (O_2) and nitrogen (N_2) are used to grow a PSG-layer acting as a phosphorus diffusion source. After the first plateau, the $POCl_3$ supply is stopped, whereas the oxygen gasflow is increased. The increased availability of oxygen and the high temperature of a second temperature plateau allow for interface oxidation between the previously grown PSG-layer and the silicon surface. Thus, P-diffusion from PSG into silicon is decelerated. During the second temperature profile, the phosphorus concentration near the silicon surface decreases whereas the depth of the doped areas increases.

3.2 Process evaluation

Symmetrical samples are prepared on Cz-wafers with an edge to edge length of 156 mm. Samples for FSF-evaluations feature alkaline textured surfaces and are wet chemically cleaned and diffused in several $POCl_3$ processes. Samples for evaluation of interface oxidation are damage etched, cleaned, PECVD-coated with BSG on both sides of the wafer, and diffused in selected $POCl_3$ processes. The investigated $POCl_3$ processes include a variation of the oxygen gas flow during the first and the second temperature plateau as well as a variation of the dwell time during the first temperature plateau.

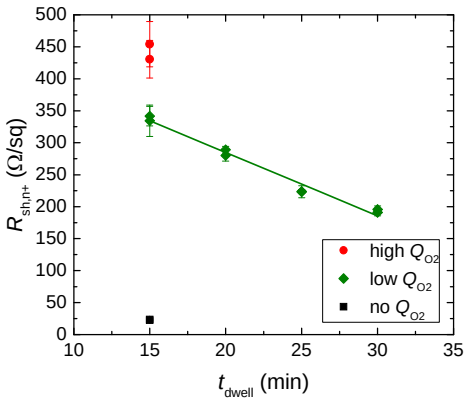

Figure 3: Sheet resistance ($R_{sh,n+}$) versus dwell time (t_{dwell}) for three different oxygen gas flows (Q_{O2}) during heating from the first to the second temperature plateau. The schematic cross section in the upper right corner depicts the sample setup. The PSG-layer forms during the diffusion process.

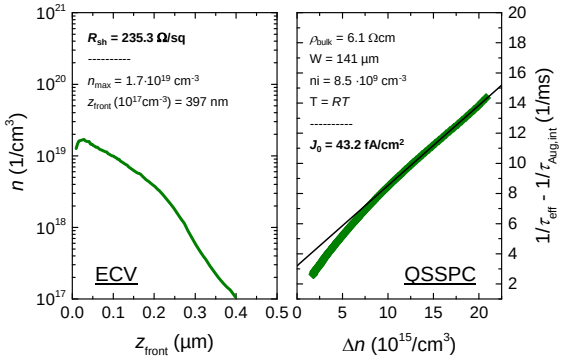

Figure 4: Electron concentration (n) versus wafer depth (z_{front}) measured by ECV on the left and inverse effective life time versus excess carrier density (Δn) measured by QSSPC on the right hand side.

Figure 3 depicts the dependence of the P doping-level expressed by the inductively measured sheet resistance $R_{sh,n+}$ in dependence of the dwell time t_{dwell} during the first temperature plateau. For t_{dwell} = 15 min also three different oxygen gas flows (Q_{O2}) during the heating phase from the first to the second temperature plateau are investigated. Here, a strong correlation is detectable. No oxygen gas flow leads to P-doped surfaces with a sheet resistance of around 25 Ω/sq. Such high doping-levels would lead to extremely high surface recombination [12] and a very low auger life time [13] and are, thus, not suitable for FSF-applications. High oxygen gas flows

enable doped surfaces with sheet resistances up to 450 Ω/sq. As described above, this increase in sheet resistance is caused by an oxidation of the interface between the grown PSG and the doped silicon surface. Regarding the sheet resistance versus dwell time for a low oxygen gas flow, a linear decrease in sheet resistance with increasing dwell time is detectable. Sheet resistances from 190 to 340 Ω/sq are adjustable with a sensitivity of approximately 10 Ω/(sq·min). These doping-levels are perfectly suitable for FSF-application.

Fig 4 shows the electron concentration profile of a selected sample (low Q_{O2}, $R_{sh,n+}$ = 235 Ω/sq) measured by electrochemical capacitance voltage (ECV). The dark saturation current density (J_0) of a sample featuring similar doped surfaces and the front side passivation of the cell device is depicted on the right hand side. J_0 is measured according to the slope method proposed in [14]. The J_0 of 43 fA/cm^2 indicates a high passivation quality of the P-doped surfaces perfectly suitable for FSF-applications.

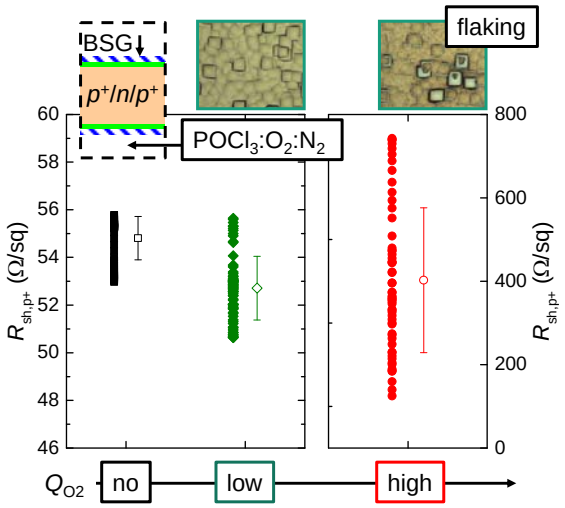

Figure 5: Sheet resistance ($R_{sh,p+}$) of doped surfaces diffused from pre-deposited BSG-versus oxygen gas flow (Q_{O2}) during heating from the first to the second temperature plateau. The schematic cross section in the upper left corner depicts the sample setup. The microscope images indicate the top view on BSG-layers after diffusion for low and high Q_{O2}.

Figure 5 depicts the dependence of the sheet resistance ($R_{sh,p+}$) diffused from pre-deposited BSG on the oxygen gas flow (Q_{O2}) during heating from the first to the second plateau. Single solid points correspond to measurement points distributed over the wafer surface. Hollow points with error bar indicate the calculated mean with standard deviation. Both representations describe the homogeneity of the diffused emitter along the wafer. By comparing the sheet resistance of emitters diffused with no (54.8 ± 0.9 Ω/sq) and low (52.7 ± 1.3 Ω/sq) oxygen gas flows, no significant difference is observable. In both cases, the relative standard deviation is below two percent, indicating the homogeneously diffused emitters. In case of a high oxygen gas flow, both, the sheet resistance and the relative standard deviation increase drastically. Additionally, a flaking of BSG is recognized. The latter observations are interpreted as a proof for the growth of silicon oxide between pre-deposited diffusion sources and the silicon surface in the case of diffusion processes featuring a high oxygen gas flow. To enable conditions which allow for FSF- and emitter formation, $POCl_3$ based co-diffusion processes must be performed with low oxygen gas flows.

3.3 Cell preparation and results

The solar cells were processed according to the base line process depicted in Figure 1. To evaluate the impact of $POCl_3$ based co-diffusion processes on the cell performance, the co-diffusion was carried out featuring either a low or a high oxygen gas flow during the first and the second temperature plateau. Table I shows the IV-data (one sun) versus oxygen gas flow (Q_{O2}) with the open circuit voltage (V_{OC}), the short circuit current density (J_{SC}), the fill factor (*FF*), the pseudo fill factor (p*FF*, [15]) and the conversion efficiency (η) as well as the ideal fill factor (FF_0, [16]).

Table I: Cell parameters (one sun) of comparable cells processed with co-difusion processes including $POCl_3$ as gaseous diffusion source for FSF-formation. The cell parameters are presented in dependence of the oxygen gas flow during the first and the second temperature plateau (Q_{O2}).

Q_{O2}	V_{OC} (mV)	J_{SC} (mA/cm^2)	*FF* (%)	p*FF* (%)	FF_0 (%)	η (%)
High	598.5	38.5	62.1	70.5	82.9	14.3
Low	653.3	40.4	77.8	80.2	83.9	20.5*

*calibrated measurement of the Fraunhofer ISE calibration laboratory

Compared to solar cells processed with a high oxygen gas flow, the optimized process with a low oxygen gas flow allows for reasonable cell parameters with a solar cell efficiency of 20.5 %. It is assumed that the cells based on a high oxygen gas flow suffer due to the already mentioned interface oxidation between silicon and the solid B-diffusion sources. The interface oxidation induces a deceleration of B-diffusion and, thus, an emitter with a low doping-level. In consequence, the contact resistance of the Al-Si/p^+-Si contact as well as the shunting current increase. The high contact resistance is confirmed by regarding the difference between p*FF* and *FF*, which correlates with the series resistance of the cell. The increase in shunting probability is confirmed by regarding the difference between FF_0 and p*FF* which indicates on shunting paths and/or high recombination in the space charge region. The lower passivation quality of the rear surface and the increase in shunting current of the cell based on a low oxygen gas flow lead to a comparably low V_{OC}.

Compared to previous results (η = 18.3 %; [17]), $POCl_3$ based BC-BJ solar cells feature an improved conversion efficiency and a strongly reduced process effort.

4 EFFICIENCY IMPROVEMENT

4.1 Motivation and cell preparation

Parallel to the work focusing on $POCl_3$ based co-diffusion processes, improvements of the base line without $POCl_3$ are carried out by using PSG as FSF-diffusion source (Route A, Figure 1). These improvements cover the introduction of an improved BSG-deposition process [8], the usage of Cz-substrates with a base resistivity below 3 Ωcm and a bulk carrier

lifetime higher than 3 ms, as well as an adaption of the contact opening coverage (COC).

As a reference process with highly industrial relevance, an inkjet-printed boron ink (B-Ink) is applied as diffusion source for emitter formation as well.

The COC of the squarely shaped contact openings is chosen to be 2 %. Since the specific contact resistance at the interfaces Al-Si/n^+-Si and Al-Si/p^+-Si is determined to be lower than 1 mΩcm^2, *FF*-losses arising from the contact resistance should not become more than 1 %$_{abs}$. To derive the upper limt of the p*FF* independent of spiking effects, reference cells without contact openings in the active cell area were prepared. Such cells feature a p*FF* slightly higher than 82 %. Thus, solar cells exceeding a p*FF* of 82 % should not be limited by spiking.

4.2 Cell results

The cell parameters of the manufactured solar cells (depicted in table II) reveal a significant increase in cell efficiency.

Table II: Cell parameters (one sun) of solar cells based on the regarded cell improvements in dependence of the diffusion source used for emitter formation. Since the solar cells feature a different passivation quality upon the emitter, the pitch distance of the cells in not comparable.

Source	V_{OC} (mV)	J_{SC} (mA/cm^2)	*FF* (%)	p*FF* (%)	η (%)
BSG	662.5	41.5	78.5	82.1	21.6*
B-Ink	654.6	41.5	76.0	80.0	20.6*

* calibrated measurement under investigation; current *EQE*-confirmed

Compared to previous results the cells based on the cell improvements feature an increase in all cell parameters. The increase in V_{OC} is assumed to be mainly generated by a decrease in emitter and contact recombination. The comparably high J_{SC} is caused by the high minority collection ability of the solar cell device featuring a high bulk carrier lifetime and an emitter coverage of around 80 %. The increase in *FF* is mainly caused by an increase in p*FF* (less spiking) and an increase in lateral conductivity (lower specific base resistivity) of the solar cell device.

Solar cells based on B-inks reveal a maximum conversion efficiency of 20.6 %. The decrease in V_{OC} is mainly caused by the cell design implying a decrease in emitter coverage. The increase of shunting currents is unclear and will be investigated in subsequent experiments.

All described improvements are transferable to the process sequence with $POCl_3$-based co-diffusion processes (route B, Figure 1). Thus, further increase in efficiency is expected for this approach as well.

5 CONCLUSIONS

BC-BJ solar cells processed according to the suggested base line process provide both, high conversion efficiencies above 21 % and a low process effort. Due to the sophisticated co-diffusion, only one high temperature step is necessary to process BC-BJ solar cell devices featuring three differently doped areas.
A severe process simplification is obtained by integrating $POCl_3$ as gaseous diffusion source for FSF-formation. The evaluated co-diffusion processes allows for P-doped surfaces with sheet resistances in the range of 190 to 340 Ω/sq and low dark saturation current densities below 45 fA/cm^2. BC-BJ cells based on these new processes allow for conversion efficiencies up to 20.5 %. Crucial issues of $POCl_3$ based co-diffusion processes like the interface oxidation of solid diffusion sources could be circumvented by carefully adjusting oxygen gas flows.

A remarkable cell improvement is achieved by integrating new B-diffusion sources, by adapting properties of the bulk material and by modifying the cell design. Within only one year, the conversion efficiency of industrially convertible BC-BJ solar cells produced using one single thermal process could be increased from 18.3 % up to 21.6 %. The steady increase in cell efficiency indicates the straight forward cell development of this sophisticated solar cell type. As an alternative to plasma based deposition techniques, direct inkjet-printing of boron inks is integrated in the base line process. In a first experiment, cells with a conversion efficiency of 20.6 % could be fabricated. To our knowledge, this is the highest conversion efficiency ever reached in case of solar cells which use printable diffusion sources.

Future research will concentrate on transferring the improvements to $POCl_3$-based co-diffusion processes for combining minimum process effort with high efficiency. The upscaling of BC-BJ solar cells from small-scale to large-scale BC-BJ solar cells will be of special interest as well.

6 ACKKNOWLEDGEMENTS

This work was supported by the project “HERCULES” which has received funding from the European Union’s Seventh Programme 217 for research, technological development and demonstration under grant agreement No. 608498.

7 REFERENCES

[1] S. Nold, *et al.*, "Cost modelling of silicon solar cell production innovation along the PV value chain," in *Proceedings of the 27th European Photovoltaic Solar Energy Conference and Exhibition*, Frankfurt, Germany, 2012, pp. 1084-90.

[2] C. del Canizo, *et al.*, "Crystalline silicon solar module technology: towards the 1€ per watt-peak goal," *Progress in Photovoltaics: Research and Applications*, vol. 17, pp. 199-209, 2009.

[3] D. D. Smith, *et al.*, "SunPower's Maxeon Gen III solar cell: high efficiency and energy yield," in *Proceedings of the 39th IEEE Photovoltaic Specialists Conference*, Tampa, FL, USA, 2013, pp. 0908-13.

[4] D. Biro, *et al.*, "PV-Tec: retrospection to the three years of operation of a production oriented research platform," in *Proceedings of the 24th European Photovoltaic Solar Energy Conference*, Hamburg, Germany, 2009, pp. 1901-5.

[5] A. Fallisch, *et al.*, "Analysis of phosphorus-doped silicon oxide layers deposited by means of PECVD as a dopant source in diffusion

processes," *IEEE Journal of Photovoltaics*, vol. 2, pp. 450-6, 2012.

[6] N. Mingirulli, *et al.*, "Hot-melt inkjet as masking technology for back-contacted cells," in *Proceedings of the 34th IEEE Photovoltaic Specialists Conference*, Philadelphia, 2009, pp. 1064-8.

[7] R. Keding, *et al.*, "Diffusion and characterization of doped patterns in silicon from prepatterned boron- and phosphorus-doped silicate glasses," in *Proceedings of the 26th European Photovoltaic Solar Energy Conference and Exhibition*, Hamburg, Germany, 2011, pp. 1385-9.

[8] R. Keding, *et al.*, "Silicon doping performed by different diffusion sources aiming co-diffusion," in *Proceedings of the 27th European Photovoltaic Solar Energy Conference and Exhibition*, Frankfurt, Germany, 2012, pp. 1906-11.

[9] J. Seiffe, *et al.*, "Surface passivation of crystalline silicon by plasma-enhanced chemical vapor deposition double layers of silicon-rich silicon oxynitride and silicon nitride," *Journal of Applied Physics*, vol. 109, p. 034105, 2011.

[10] A. Richter, "Aluminum oxide for the surface passivation of high efficiency silicon solar cells - Technology and advanced characterization," Dissertation, Fraunhofer Institut für Solare Energiesysteme (ISE), Universität Konstanz, Freiburg, 2014.

[11] F. Granek, *et al.*, "Front surface passivation of n-type high-efficiency back-junction silicon solar cells using front surface field," in *Proceedings of th 22nd European Photovoltaic Solar Energy Conference* Milan, Italy, 2007, pp. 1454-7.

[12] A. Cuevas, *et al.*, "Surface recombination velocity of highly doped n-type silicon," *Journal of Applied Physics*, vol. 80, pp. 3370-5, 1996.

[13] P. P. Altermatt, "Models for numerical device simulations of crystalline silicon solar cells—a review," *Journal of Computational Electronics*, vol. 10, pp. 314-30, 2011.

[14] A. Cuevas and D. Macdonald, "Measuring and interpreting the lifetime of silicon wafers," *Solar Energy*, vol. 76, pp. 255-62, 2004.

[15] R. A. Sinton and A. Cuevas, "Contactless determination of current-voltage characteristics and minority-carrier lifetimes in semiconductors from quasi-steady-state photoconductance data," *Applied Physics Letters*, vol. 69, pp. 2510-2, 1996.

[16] M. A. Green, *Silicon Solar Cells Advanced Principles & Practice* vol. 1-364: Centre for Photovoltaic Devices and Systems University of New South Wales Sydney, N.S.W. 2052, 1995.

[17] R. Keding, *et al.*, "Co-diffused back-contact back-junction silicon solar cells," in *Proceedings of the 28th European Photovoltaic Solar Energy Conference and Exhibition*, Paris, France, 2013, p. to be published.